Determination of the Influences of Deteriorated Track Conditions on Gauge Widening in Concrete Sleeper Track

Josué C. Bastos[1, 2], Marcus S. Dersch[1], J. Riley Edwards[1], and Bassem O. Andrawes[3].

[1] Rail Transportation and Engineering Center - RailTEC. Department of Civil and Environmental Engineering. University of Illinois at Urbana-Champaign. Urbana. Illinois. USA.

[2] CAPES Foundation. Ministry of Education of Brazil. Brasilia, DF 70.040-020. Brazil.

[3] Department of Civil and Environmental Engineering. University of Illinois at Urbana-Champaign. Urbana. Illinois. USA.

Contact: jedward2@illinois.edu

Abstract

Improper track geometry can lead to derailments with severe consequences, thus avoiding such geometric deviations is a priority in ensuring safe railway operation. In the North American railway network, derailments have been caused by gauge widening due to deteriorated concrete sleepers and fastening systems, despite the fact that concrete sleepers generally hold gauge better than timber sleepers. Similarly, a review of literature shows that sleeper cracking from center binding is among the most critical concrete sleeper and fastening system problems internationally. As ballast support conditions are critical to sleeper performance, there is a need to fully understand the behavior of these poorly supported sleepers. To quantify the influence of support conditions on sleeper deflection and propose a methodology to predict gauge widening, laboratory experiments were performed at the University of Illinois at Urbana-Champaign. Using a static structural loading frame, new and cracked concrete sleepers were subjected to different supporting conditions through the use of rubber pads. Simulated conditions included center bound sleepers, newly tamped track, and track under high impact loads. Poor support can force sleepers to bend and crack when subjected to high loads, which potentially makes the track more prone to geometry deviations, including gauge widening. This paper presents a correlation between ballast support conditions, structural health of concrete sleepers, and their effect on track gauge. Using statistical tools, it is shown that there is no significant difference between experimental results of new and cracked sleepers. In addition, the gauge widening effect due to pure concrete sleeper bending seemed to be minimal.

1. Introduction

In the United States, more than 25% of the railway accidents on Class I railroad mainlines are caused by defective infrastructure conditions, which frequently result in gauge widening in both timber and concrete sleeper track (Bastos 2015). Gauge widening is typically caused by rail wear, rail roll, worn fastening systems, rail cant deficiency, broken sleepers, or bent sleepers, contributing to wheel-drop derailments, especially in the presence of worn wheels (Wu 2006). This study focuses on quantifying the gauge widening effect due to concrete sleeper bending for different support conditions and sleeper center cracks.

1.1 Experimentation Plan

Laboratory experiments were performed at the Rail Transportation and Engineering Center's (RailTEC) Research and Innovation Laboratory (RAIL) in Champaign, Illinois, USA, to quantify the influence of support conditions and light sleeper center cracking on gauge widening due to concrete sleeper bending. Individual concrete sleepers were placed in a steel loading frame where both rail seats could be simultaneously loaded in the vertical direction. The sleepers were supported by different arrangements of rubber pads, simulating uniform ballast layer, center binding, newly tamped track, and track with high impact wheel loads. All of the pads were one inch (25.4 mm) thick, 12 inches (304.8 mm) wide, and 12 inches (304.8 mm) long, with a hardness of 50 shore A durometer. The authors were comfortable with the use of rubber pads as the sleeper vertical displacements measured at the laboratory were in the range of 0.05 to 0.1 inches (12.7 to 25.4 mm) under 20 kip (89 kN) loading at both rail seats, numbers comparable to recorded displacements measured in the field (Manda 2014). To quantify the vertical displacement along the sleeper span, linear potentiometers (voltage differential transducers) were used. Each sleeper was monitored with 15 potentiometers: one at the sleeper center and seven symmetrically located on each side. Similarly, the support and loading conditions used in this experiment were always symmetric. Having both sides of the sleeper instrumented increased the sample size to further account for the variability associated with different support and sleeper conditions.

Both rail seats of a single sleeper were simultaneously loaded with equal vertical forces up to 20 kips (89 kN). A wheel load of 40 kips (177.9 kN) provides an approximate representation of the 95th percentile nominal wheel load for loaded freight cars in the US, based on a representative sample of railcars in unrestricted interchange on a Class I railroad (Van Dyk 2014). A single sleeper bears approximately 50 percent of the axle load applied directly above it assuming 24 inch (610 mm) sleeper spacing (American Railway Engineering and Maintenance-of-way Association 2014). Therefore, loading up to 20 kips (89 kN) approximates the 95th percentile nominal rail seat load imparted by a loaded freight car in the US. From the passenger service perspective, a wheel load of 40 kips (177.9 kN) represents approximately the 90th percentile of peak loads of loaded commuter railcars in the US Northeast Corridor based on a recent study on three different commuter rail systems (Lin 2015). Therefore, holding the assumption that a single sleeper bears approximately 50 percent of the axle load applied over it, loading up to 20 kips (89 kN) roughly represents the 90th percentile of peak rail seat loads that are induced by a loaded commuter rail car. For high-speed rail, however, there is limited available data on wheel loads in North America. In such case, a 13.2 kip (58.7 kN) nominal wheel load can be assumed for loaded Japanese Shinkansen rolling stock (Yanase 2010). Considering that a speed factor of three is recommended for high-speed track design (Wang 2015), then a design wheel load of 39.6 kips (176.1 kN) can be assumed, leading again to approximately 20 kips (89 kN) of rail seat load. Thus, the loading conditions used to collect data for this paper are representative of certain types of freight, commuter, and high-speed rail services.

Figure 1 illustrates the support conditions used for laboratory experimentation. The “full support” condition is the baseline scenario where a uniform and homogenous layer of ballast is represented by pads under the entire sleeper. Three variations of “center binding” were simulated in the experiments, with the most severe case having the shortest length of support pads under the sleeper center. The arrangement for “lack of rail seat support” takes into consideration the fact that, under field conditions, the ballast below the rail seat typically degrades faster than other areas under the sleeper due to impact loads resulting from track or wheel irregularities. Finally, the “lack of center support” configuration assumes that the ballast does not provide significant support at the sleeper center area, which could represent newly tamped track. This condition is simulated by including pads only at the area reached by the tines of a tamping machine.

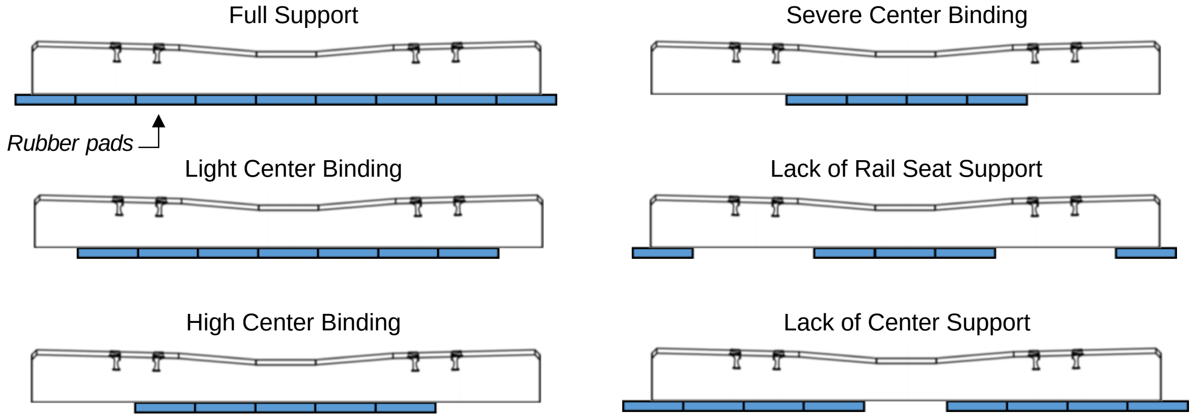

Figure 1 Experimental support conditions for concrete sleepers

All experiments were conducted five times with healthy concrete sleepers and five times with center-cracked sleepers, and all sleepers were of the same design. The cracks were generated in the laboratory by simultaneously loading both rail seats of a single sleeper with equal vertical forces up to 20 kips (89 kN) while the sleeper was supported with a severe center binding condition (Figure 1). Typically, after cracking, each sleeper presented seven horizontal cracks that were approximately symmetric about its midspan. All cracked sleepers had cracks going deeper than the first level of prestress and the deepest cracks reached approximately 3 inches (76.2 mm) below the top surface. In addition, the cracks closed up after unloading the sleepers due to the presence of prestressing material. Since each sleeper was instrumented with symmetrically-located potentiometers, ten data points were collected for each support condition per potentiometer location (except for the center one), with healthy and cracked sleepers. For statistical purposes, one replicate will be associated with half of a sleeper in this paper. Therefore, ten replicates were performed for each potentiometer location, support condition, and sleeper health condition.

2. Results of Experimentation

In order to correlate the resulting sleeper shape with a corresponding gauge widening effect when the loading and support conditions are symmetric about the sleeper midspan, Equation 1 was derived based on basic geometry concepts.

$$\frac{1}{2}\Delta g = \sqrt{2\left(l^2 + \frac{r^2}{4}\right)(1-\cos(\theta))} \times \sin\left(tan^{-1}\left(\frac{l}{r/2}\right) + \varphi - \frac{\theta}{2}\right) - \frac{w}{2}\cos(\varphi) + \frac{w}{2}\cos(\varphi - \theta) \qquad (1)$$

where,

Δg: Change of gauge due to sleeper bending.
l: Rail height at gauge measurement location.
r: Distance between the two potentiometers located by each rail.
φ: Rail cant angle.
w: The width of rail head at gauge measurement location.
θ: Induced rail rotation angle:

$$\theta = sin^{-1}\left(\frac{\Delta d \times \cot(\varphi) \times \sin(\varphi)}{\sqrt{(\Delta d \times cot(\varphi))^2 + (r - \Delta d \times csc(\varphi))^2 + 2(\Delta d \times cot(\varphi))(r - \Delta d \times csc(\varphi))(\cos(\varphi))}}\right) \qquad (2)$$

All gauge widening numbers presented in this study are based on the 136RE rail considering that track gauge is measured 5/8 inches (15.875 mm) below the top of the rail (Federal Railroad Administration 2015). Figure 2 shows the results for the different support conditions and demonstrates that the gauge widening effect due to concrete sleeper bending is small even for extreme center binding support conditions.

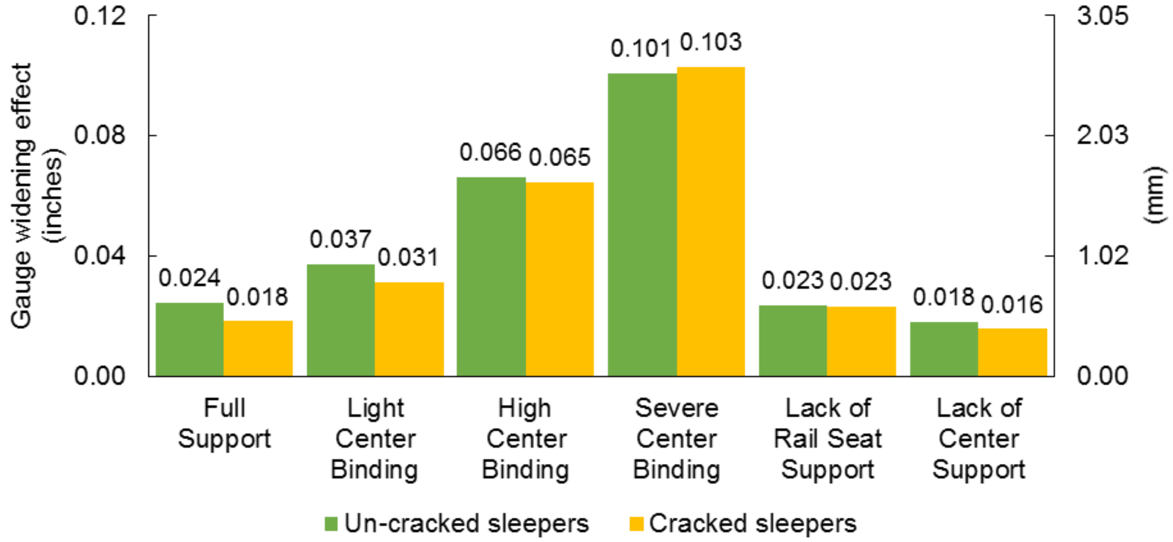

Figure 2 Gauge widening due to concrete sleeper bending at rail seat load of 20 kips (89 kN)

To guide the process of data analysis and account for experimental variability, a statistical model was developed using the concept of completely randomized design (CRD) with two factors, as shown in

Equation 3 (Ott 2008). The same model was used for the three locations (rail seat, center, and intermediate) and the rail seat load was fixed at 20 kips (89 kN). For easier reading, Equation 3 uses Latin letters that are associated with their meaning (as opposed to the exclusive use of Greek letters that is typical of classical statistics):

$$\Delta g_{ijk} = \mu + s_i + c_j + sc_{ij} + \varepsilon_{ijk} \tag{3}$$

where,

Δg_{ijk}: k^{th} observation of gauge widening with the i^{th} support condition and the j^{th} sleeper health state.
μ: Grand population mean for gauge widening.
s_i: Fixed effect of the i^{th} support condition on gauge widening.
c_j: Fixed effect of the j^{th} sleeper health state on gauge widening.
sc_{ij}: Effect of interaction between the i^{th} support condition and the j^{th} sleeper health state on gauge widening.
ε_{ijk}: Random error (residual) of the k^{th} observation with the i^{th} support condition and the j^{th} sleeper health state.

To analyze the experimental results with this model, the errors must be both normally and independently distributed with equal variance (Ott 2008). As no correlation was expected to be found, the independence assumption was not formally verified. However, the other assumptions were confirmed using the Shapiro-Wilk test for normality (Shapiro 1965) and the Brown and Forsythe's test for homogeneity of variance (Brown 1974). In order to meet them, however, the gauge widening data had to be transformed (Ott 2008). Due to the relationship between mean and variance in this particular dataset, the best transformation was found to be the square root of the negative natural logarithm of the data. The homogeneity of variance and normality assumptions were met at significance levels of 0.2685 and 0.1200, respectively.

As previously discussed, ten replicates were obtained for each case. With the measured mean square error (MSE), the confidence interval for the population mean was estimated using Equation 4, which is derived from the Central Limit Theorem (Ott 2008). Using the MSE, the deviation of the sample means relative to the respective population means is no greater than 0.01 in (0.254 mm) for a confidence interval of 96%.

$$n \approx \frac{(z_{\alpha/2})^2 \hat{\sigma}^2}{D^2} \tag{4}$$

where,

n: Number of observations (replicates).
$z_{\alpha/2}$: z-value from standard normal distribution.
α: Significance level.
$\hat{\sigma}^2$: Sample variance (MSE was used in this analysis).
D: Detectable deviation of sample mean relative to population mean.

The effect of center cracks and different support conditions on gauge widening due to sleeper bending were stated to be either significant or not significant based on a two-way analysis of variance (ANOVA) (Fisher 1970). Table 1 presents the ANOVA results for the gauge widening analysis, with the last column showing the p-value ("Pr > F" column) that is compared to the significance level. The interaction effect is not significant, which allows for a better interpretation of the main effects (Ott 2008). Not surprisingly, the support condition factor has a very significant effect on gauge widening due to sleeper bending. On the contrary, the sleeper health condition does not have a significant effect on the resulting numbers, meaning that the particular cracking pattern created at the laboratory does not contribute to a significant difference in gauge widening in relation to the un-cracked condition.

Table 1 ANOVA results

Source	DF	Sum of Squares	Mean Square	F Value	Pr > F
Support	5	4.4952	0.8990	66.55	<0.0001
Cracking	1	0.0178	0.0178	1.32	0.2529
Interaction support-crack	5	0.0494	0.0099	0.73	0.6017
Error	108	1.4590	0.0135		
Corrected Total	119	6.0214			

Figure 3 shows the displacement results of healthy concrete sleepers under the rail seat load of 20 kips (89 kips) relative to the center displacement. As there is no statistically significant difference between un-cracked and cracked sleepers, the results of the latter are not presented. The highest center displacement was 0.069 in (1.7526 mm) for lack of rail seat support and the lowest was 0.039 in (0.9906 mm) for high center binding.

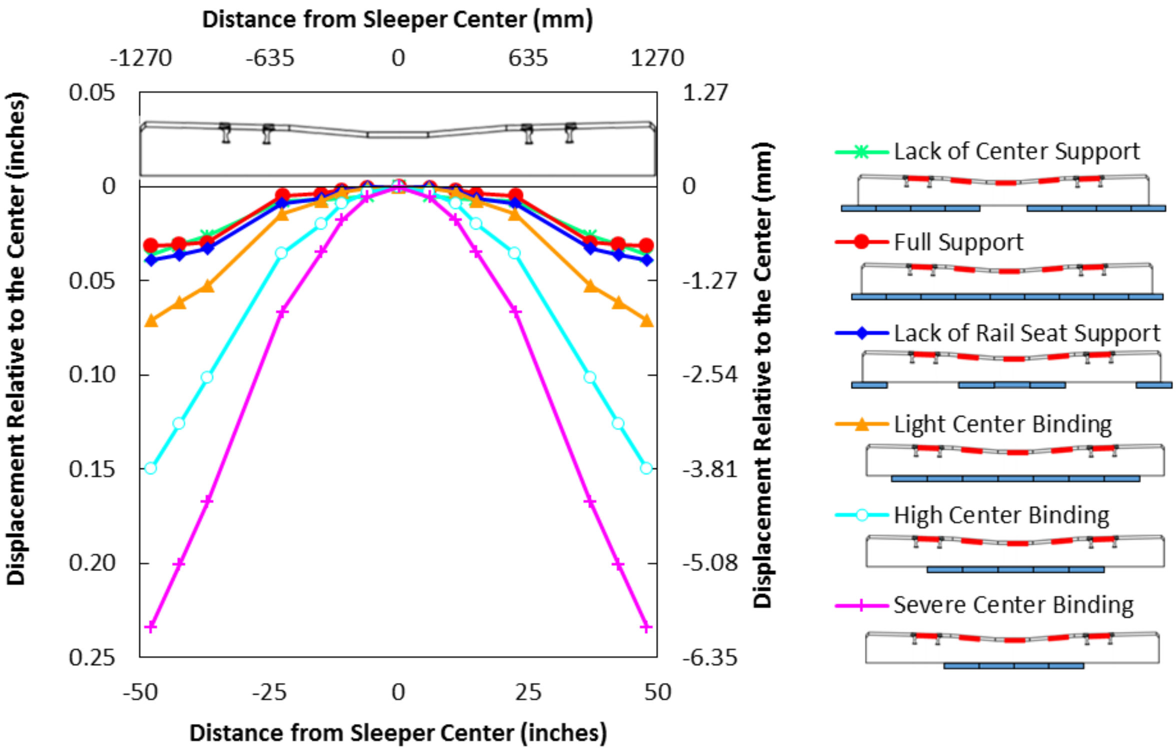

Figure 3 Average relative displacements of healthy concrete sleepers at rail seat load of 20 kips (89 kN)

3. Conclusions

Laboratory experiments were performed to quantify the influence of support conditions and sleeper cracking on sleeper deflection and an equation was derived to estimate the gauge widening due to sleeper bending. The primary findings from this research were:

- Light center cracks have no significant effect on the flexural performance of concrete sleepers (p-value less than 0.0001);
- Support conditions of concrete sleepers have a significant effect on the flexural performance of concrete sleepers (p-value of 0.25);
- Concrete sleeper bending due to center binding support conditions is minimal (maximum gauge widening of 0.103 inches (2.6162 mm)) even when light center cracks are present.

Additional research is necessary to determine the influence of more severely deteriorated conditions of concrete sleepers on its performance. However, it is clear that the track support has a major role in affecting sleeper behavior and maintaining proper support conditions and it should be of greater concern than light sleeper center cracking.

4. Acknowledgments

This research effort is funded by the Federal Railroad Administration (FRA), part of the United States Department of Transportation (US DOT). The material in this paper represents the position of the authors and not necessarily that of FRA. The authors also would like to acknowledge the following industry partners: Union Pacific Railroad; BNSF Railway; National Railway Passenger Corporation (Amtrak); Amsted RPS/ Amsted Rail, Inc.; GIC; Hanson Professional Services, Inc.; and CXT Concrete Ties, Inc., and LB Foster Company. In addition, the authors would like to extend their gratitude to the team of graduate and undergraduate research assistants for helping with this project. The authors also would like to thank Henry Wolf and Samantha Chadwick who added immeasurable value to this analysis with their expert opinion. Finally, the experimental guidance of Yu Qian, Matthew Csenge and the laboratory work of the CEE Machine Shop are gratefully acknowledged. J. Riley Edwards has been supported in part by the grants to the UIUC Rail Transportation and Engineering Center (RailTEC) from CN, Hanson Professional Services, and the George Krambles Transportation Scholarship Fund. Josué César Bastos has been supported in part by CAPES Foundation, Ministry of Education of Brazil.

References

American Railway Engineering and Maintenance-of-Way Association. 2014. *AREMA Manual For Railway Engineering*. AREMA, Landover, Maryland.

Bastos, J., M. Dersch and J.R. Edwards. 2015. Determination Of Critical Track Conditions And Their Impact On The Performance Of Concrete Crossties And Fastening Systems. In: *Proceedings Of The AREMA 2015 Annual Conference*, AREMA, Minneapolis, Minnesota, USA, 2015.

Brown, M.B. and A.B. Forsythe. 1974. Robust tests for the equality of variances. *Journal of the American Statistical Association* 69 (346): 364–367.

Federal Railroad Administration. 2015. *Track Safety Standards*.

Fisher, R.A. 1970. *Statistical Methods For Research Workers*, 14th ed., revised and enlarged ed. Oliver and Boyd, Edinburgh.

Lin, X., R. Edwards, Marcus Dersch and C. Ruppert Jr. 2015. Presentation. Load Quantification for Light Rail, Heavy Rail, and Commuter Rail Transit Infrastructure.

Manda, K.R., M. Dersch, R. Kernes, R.J. Edwards and D.A. Lange. 2014. Vertical Load Path Under Static And Dynamic Loads In Concrete Crosstie And Fastening Systems. In: *2014 Joint Rail Conference*, American Society of Mechanical Engineers, 2014.

Ott, R. and M. Longnecker. 2008. *An Introduction To Statistical Methods And Data Analysis*. Cengage Learning.

Shapiro, S.S. and M.B. Wilk. 1965. An analysis of variance test for normality (complete samples). *Biometrika*: 591–611.

Van Dyk, B. 2014. *Characterization Of The Loading Environment For Shared-use Railway Superstructure In North America*. M.S. Thesis. University of Illinois at Urbana-Champaign.

Wang, P. 2015. *Design Of High-Speed Railway Turnouts: Theory And Applications*. Academic Press.

Wu, H. and N. Wilson. 2006. 8 Railway Vehicle Derailment and Prevention. *Handbook of railway vehicle dynamics*: 209.

Yanase, N. 2010. High Speed Rolling Stock in Japan. Presentation. International Practicum on Implementing High-Speed Rail in the United States.